NOTES AND CORRESPONDENCE

Sensitivity of Teleconnection Patterns to the Sign of Their Primary Action Center

WILBUR Y. CHEN AND HUUG VAN DEN DOOL

Climate Prediction Center, NOAA/NWS/NCEP, Washington, D.C.

6 January 2003 and 19 May 2003

ABSTRACT

Teleconnection patterns have been extensively investigated, mostly with linear analysis tools. The lesser-known asymmetric characteristics between positive and negative phases of prominent teleconnections are explored here. Substantial disparity between opposite phases can be found. The Pacific–North American (PNA) pattern exhibits a large difference in structure and statistical significance in its downstream action center, showing either a large impact over the U.S. southern third region or over the western North Atlantic Ocean. The North Atlantic–based patterns display significant impacts over the North Atlantic for large positive anomalies and even larger impacts over the European sector for large negative anomalies.

The monthly variance is distributed nearly evenly over the entire North Atlantic basin. A teleconnection pattern based on different regions of the basin has been known to assume different structure and time variations. The extent of statistical significance is investigated for three typical North Atlantic–associated patterns based separately on the eastern (EATL), western (WATL), and southern (SATL) regions of the North Atlantic. The EATL teleconnection pattern is similar to the classical North Atlantic Oscillation (NAO). The WATL pattern, however, is more similar to the Arctic (Annular) Oscillation (AO). The sensitivity of the North Atlantic–based teleconnection to a slight shift in base point can be fairly large: the pattern can be an AO or an NAO, with distinctive significance structure between them. Other discernible features are also presented.

1. Introduction

Remotely teleconnected anomaly patterns have long been recognized and applied in long-range predictions. Walker and Bliss (1932) identified the North Pacific Oscillation and the North Atlantic Oscillation (NAO). Lorenz (1951) noted a zonally symmetric seesaw between sea level pressures in polar and temperate latitudes. O'Connor (1969) and Namias (1981) generated a series of teleconnection atlases covering the whole Northern Hemisphere and applied the results in extended-range forecasts. Wallace and Gutzler (1981) systematically documented the recurrent standing oscillations while providing physical meanings and coined the name of a frequently recurrent teleconnection over the North Pacific–North American region as the Pacific–North American (PNA) pattern. A series of in-depth studies of structures and time variations of teleconnections was then conducted by Blackmon et al. (1984a,b) and Kushnir and Wallace (1989). The prominence of a score of teleconnection patterns was also documented by Mo and Livezey (1986), Barston and Livezey (1987), and Van den Dool et al. (2000).

Corresponding author address: Dr. Wilbur Y. Chen, Climate Prediction Center, National Centers for Environmental Prediction, 5200 Auth Road, Camp Springs, MD 20746.
E-mail: wilbur.chen@noaa.gov

Over recent decades, the NAO has been found to oscillate not only from week-to-week but also from month-to-decadal timescales (Deser and Blackmon 1993; Kushnir 1994; Hurrell 1995a,b; 1996; Walsh et al. 1996; Nakamura 1996; Kushnir et al. 1997; Shabbar et al. 1997; Hurrell and van Loon 1997; Visbeck et al. 1998). Recently, Thompson and Wallace (1998, 2000) suggested that the NAO might be thought of as part of a symmetric ''annular'' mode of variability, the Arctic Oscillation (AO), which is characterized by a seesaw of atmospheric mass between the polar cap and the midlatitudes in both the Atlantic and Pacific Oceans. Baldwin and Dunkerton (1999) addressed the propagation of the AO from the stratosphere to the troposphere. Ambaum and Hoskins (2002) established the relationship among surface pressure variation associated with the NAO, tropopause height, and the strength of the stratospheric vortex.

Rich information has been gathered and a fairly comprehensive understanding has been gained. However, the revealed teleconnection pictures appear to be linear in characteristic, since most of the studies are investigated by linear tools, such as the contemporaneous or lagged correlation analysis, or, empirical orthogonal function or singular value decomposition analysis. In this note, we investigate how linear the teleconnections are. We attempt to study the lesser-known nonlinear (asymme-

try) characteristics and the sensitivity of teleconnections to the sign of their primary action centers as well as to base-point perturbations. In addition to nonlinear behavior, possible differences in statistical significance of the teleconnection structure are also examined.

2. Data used and analysis technique

The data used are the 500-mb geopotential heights (Z500). They were extracted from the National Centers for Environmental Prediction–National Center for Atmospheric Research (NCEP–NCAR) reanalysis (Kalnay et al. 1996). Since the boreal winters showed largest variability and clearest teleconnection patterns over the extratropical latitudes (e.g., Blackmon et al. 1984a; Kushnir and Wallace 1989), we choose to analyze the wintertime teleconnections only. Although the NCEP–NCAR reanalysis has been available since 1949, we utilize only the period from 1971 to 2001, for no particular reason other than that we are comfortable with this period. It is long enough to yield statistically significant results, as will be shown later, and it is close to the new period (from 1971 to 2000) for a 30-yr climatology calculation recommended by the World Meteorological Organization. The geographical distribution of standard deviation obtained for this period, wherein its maxima constitute our bases of teleconnection studies, can also be compared with that from an earlier period used by Blackmon et al. (1984a) and Kushnir and Wallace (1989).

The geographically fixed teleconnection patterns are our main concern in this note. Since they have been shown by Blackmon et al. and Kushnir and Wallace to show up mainly in monthly means or longer timescales, we choose to analyze only the monthly mean data. An extended wintertime from 1 December to 31 March (DJFM) was considered here. A 31-day low-pass running mean filter was applied to the daily data to focus on the monthly means. The data used prior to filtering were therefore from 16 November to 15 April. Also, although we have 121 low-pass-filtered data points for each DJFM season, there are only about 4 independent data points. With 31 yr of Z500 considered, we have therefore about 31×4 ($=124$) independent data points, which is believed to contain large enough degrees of freedom to yield statistically significant results.

In order to find out whether the nonlinear characteristics in teleconnections are an important consideration, we take a different approach than most of the previous investigators. Instead of using a linear analysis tool, we employ the ''composite,'' so that a separate positive and negative phase of teleconnection can be obtained and contrasted. In addition to the composite, an evaluation of uncertainty around the composite is also conducted. The composite and the uncertainty lend us a way to determine the statistical significance of the resulting teleconnection composite.

According to sampling theory (e.g., Morrison 1983), a z score statistic Z, at any given grid point, can be defined as follows:

$$Z = C/S/\mathrm{sqrt}(N), \tag{1}$$

where C is the composite mean (the average of selected anomalies), S the standard deviation about C, sqrt the square root, and N the number of independent maps used for estimating C and S. As mentioned earlier, we have about 124 independent maps. The theoretical distribution of Z here should therefore be close to normal (Gaussian), and the corresponding critical value of Z for a 95% (99%) confidence level is 1.96 (2.58). In this note, we report these 95% and 99% confidence levels of statistical significance based on these critical values instead of basing them on a Student's t test used for a small sample.

3. Results

a. Primary action centers

Atmospheric fluctuations consist of all timescales. Blackmon et al. (1984a) show that not all timescales lead to development of geographically fixed teleconnections, which are our main concern for this note. They show that 2.5–6-day short timescales yield propagating baroclinic waves, and 10–30-day intermediate timescales produce zonally oriented mobile wave trains. For geographically fixed teleconnections, one is advised to look into 30-day means or longer timescales. We therefore concentrate only on the monthly means. Figure 1 repeats the evaluation of geographical distribution of standard deviation (std dev) for the monthly mean Z500 data. The presentation of the std dev chart is important to clarify 1) the four regions used in this investigation (each region has a variance maximum and, as such, is considered to be the primary action center for its associated teleconnection pattern) and 2) the domain used for constructions of the composite and significance level. Meanwhile, there are minor differences between this std dev chart and the one from Blackmon et al. (1984a; their Fig. 2). While our std dev maximum over the North Atlantic is located east of southern Greenland and north of 60°N, theirs is located south of 60°N. Our std dev chart shows a significant maximum in western Russia, while theirs does not have this maximum. These differences possibly result from the different periods being investigated. Ours is from 1971 to 2001, and theirs is from 1963 to 1980.

As shown by previous investigators, a teleconnection pattern can be obtained based on any grid point. In our analysis here we consider only those based on regions where a maximum std dev can be found. The rationale is that the primary action center of a teleconnection is where the maximum std dev is located. Taking the PNA teleconnection for instance, as shown in Fig. 1, there is not nearly as high a variance in the two downstream-center areas. Another consideration is the direction the

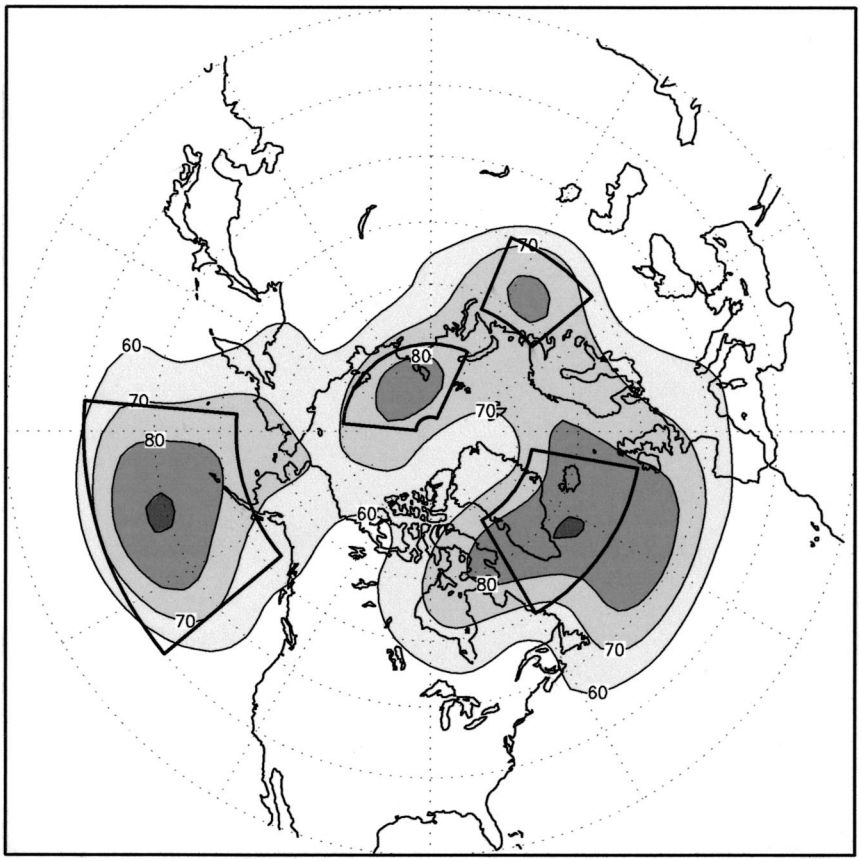

FIG. 1. Distribution of standard deviations of Z500 30-day means, evaluated for the extended wintertime season, 1 Dec–31 Mar, for the period 1971–2001. The heavy solid lines box the latitudes and longitudes for construction of teleconnection composites. Details can be found in the text and in Figs. 2–5.

energy disperses (e.g., Blackmon et al. 1984b). Since energy disperses downstream, it is not much help to look at a base point downstream of the maximum-variance area.

There are four std dev maxima in Fig. 1. We would like to see the extent of asymmetrical behavior of each teleconnection pattern based on each of these four maxima. As mentioned earlier, we rely on composites of both phases based on a std dev maximum. To construct a composite and the associated statistical significance, we apply two constraints: 1) select only those anomalies with absolute magnitude exceeding 100 m and 2) restrict the searching area to the domain, as indicated in Fig. 1 (details with given figure). It is important to mention that the sensitivity of selecting a different threshold for criteria 1) and 2) is not large enough to lead to a different conclusion.

b. Sensitivity of PNA teleconnections

The domain in the North Pacific selected for constructing the PNA teleconnection composites, as shown in Fig. 1, is 35°–57.5°N, 175°E–140°W, covering most of the region with std dev values larger than 70 m and with the maximum std dev near the center of this domain. When a monthly mean Z500 anomaly at a grid point within this domain is larger than 100 m (smaller than −100 m), then the whole global Z500 field is used for the construction of the positive (negative) PNA composite. Among the 3751 (121 × 31) overlapping monthly Z500 maps, 1686 (1601) met the two criteria imposed above and went into the construction of the positive (negative) composite. The results are shown in Figs. 2a and 2b. A PNA pattern associated with the North Pacific std dev maximum can be clearly seen. There are differences between the positive and negative composites, which will be addressed below.

The same selected maps are also used for the evaluation of the uncertainty around their mean. Since we have the mean, which is the composite itself, it is easy to get the standard deviation from the mean. The variance thus obtained is a measure of uncertainty (natural variability) that will help shape the statistical significance of the composite. The results obtained are shown in Figs. 2c and 2d. They are largely similar, yet careful examination can reveal some differences, especially

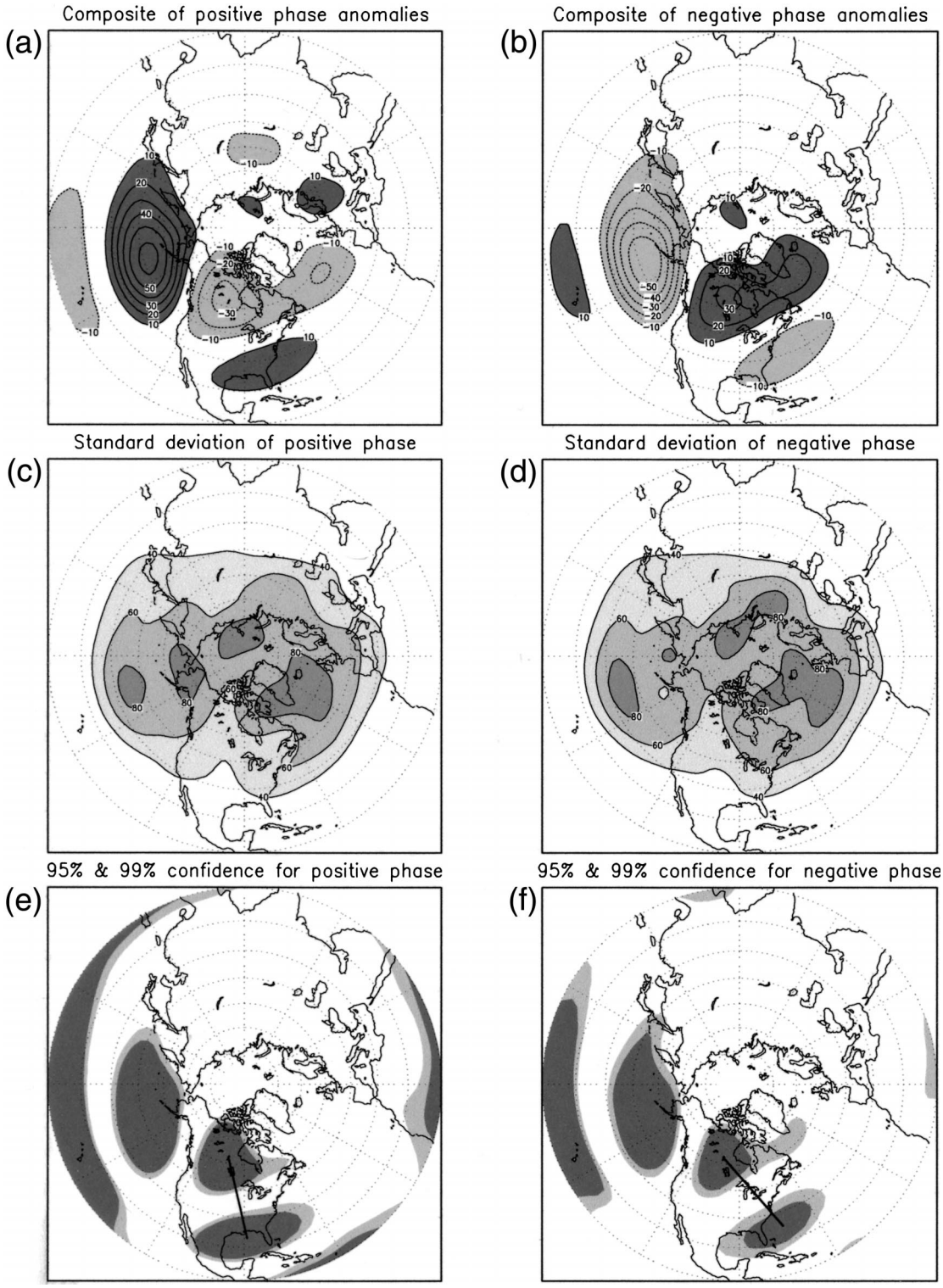

FIG. 2. Sensitivity of PNA teleconnection pattern to a phase-of-action center located in North Pacific. The domain used for obtaining these results, as marked in Fig. 1, is 35°–57.5°N, 175°E–140°W. (a),(b) Composites when the magnitude of the anomaly within the box exceeds 80 m; the unit is m. Darker shade represents positive composite and lighter represents negative. (c), (d) The unit is m. (e), (f) Contours are dimensionless, ranging from 0.0 to 1.0.

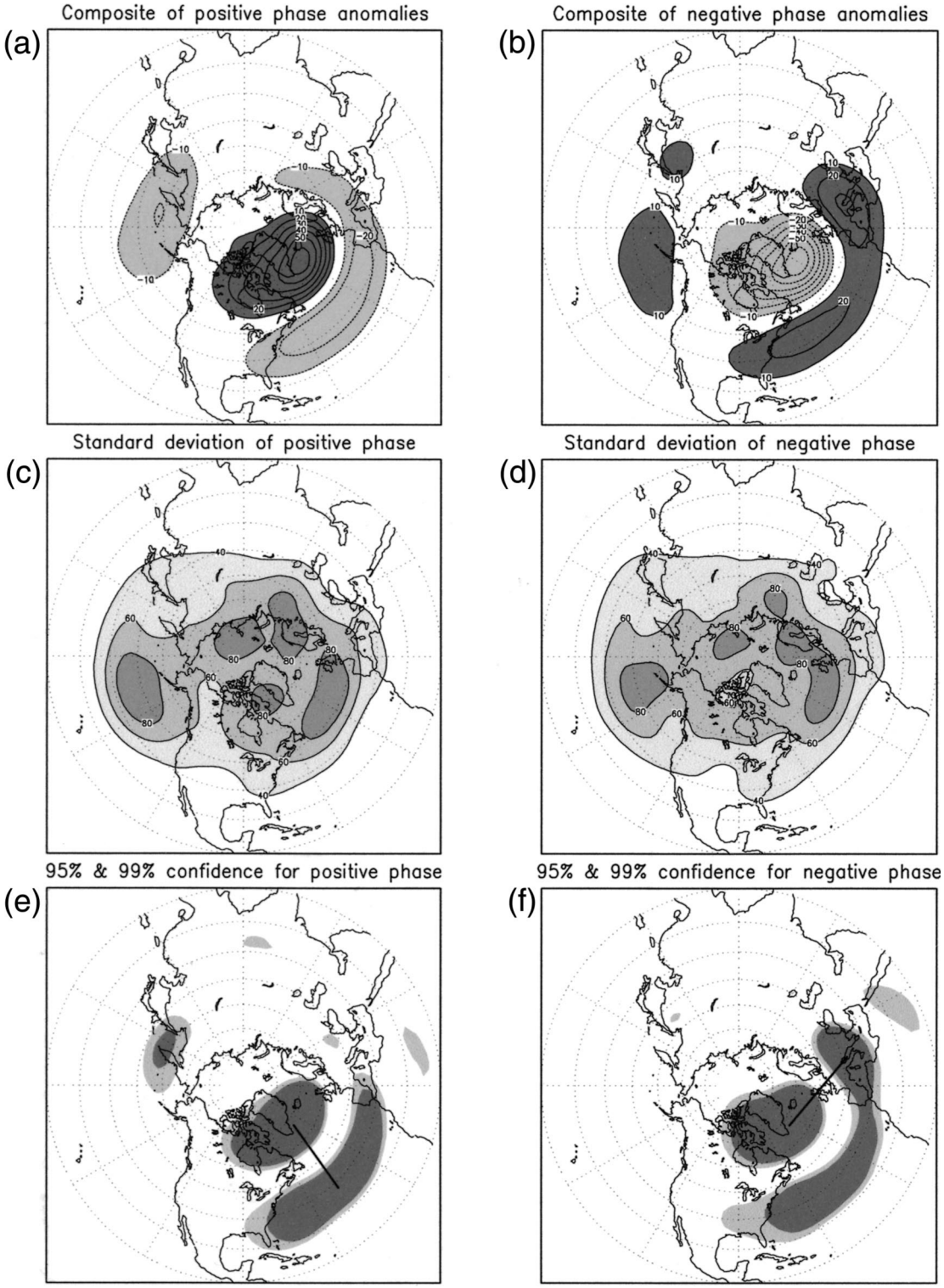

FIG. 3. The same as Fig. 2 except for an action center located in the North Atlantic. The domain, as marked in Fig. 1, is 55°–75°N, 60°–10°W.

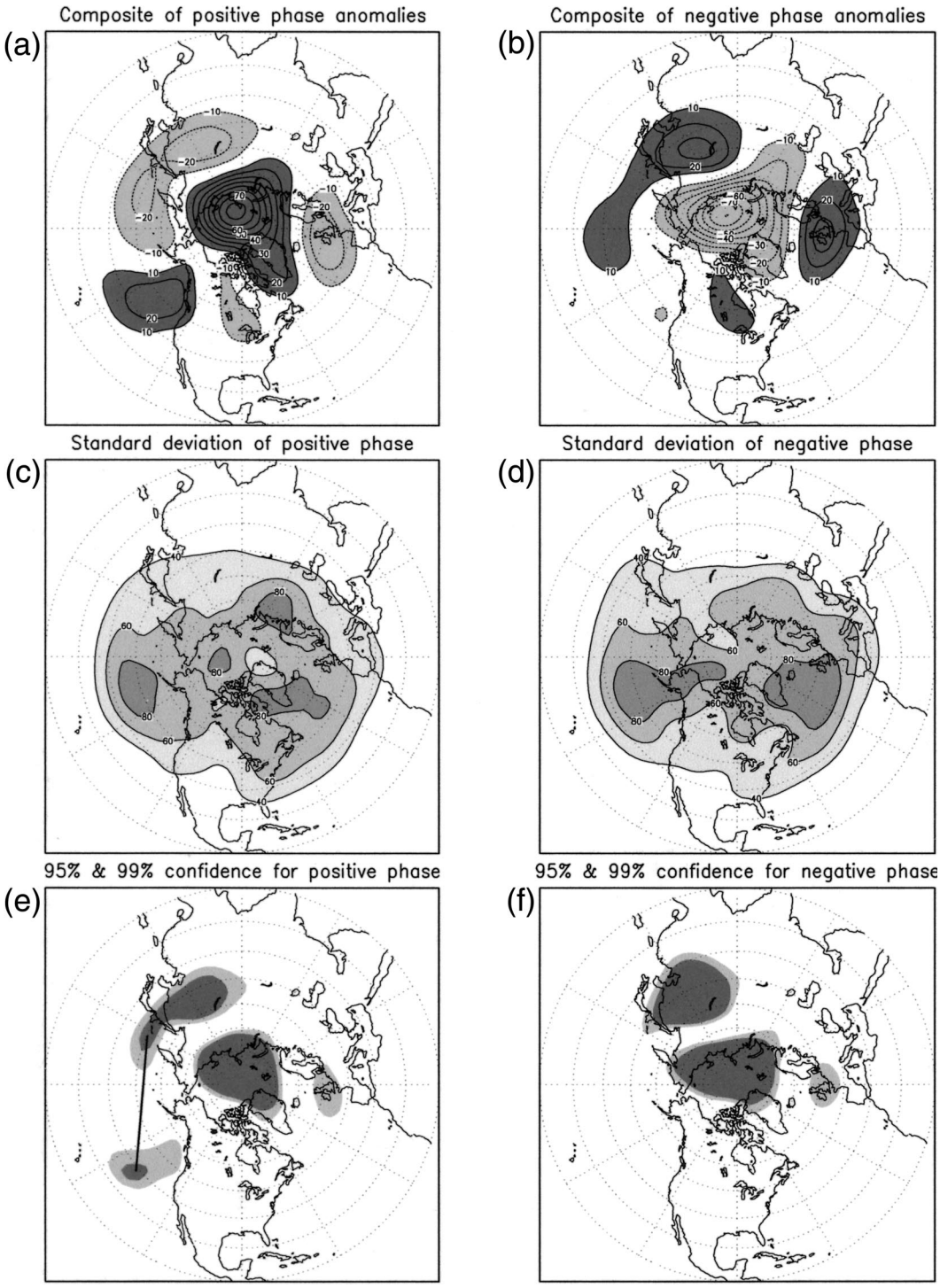

FIG. 4. The same as Fig. 2 except for an action center located near the Arctic. The domain, as marked in Fig. 1, is 75°–87.5°N, 65°–175°E.

around the variance maximum, which the composites are based on. Using formula (1), the statistical significance of the resulting teleconnections is evaluated and shown in Figs. 2e and 2f. As seen in these two panels, a large region around the original std dev maximum has a confidence level beyond 99%, as expected. Large areas around the other three action centers also show confidence levels beyond 99%. However, a disparity is also prominently exhibited by the downstream action center. The major difference between the positive and negative

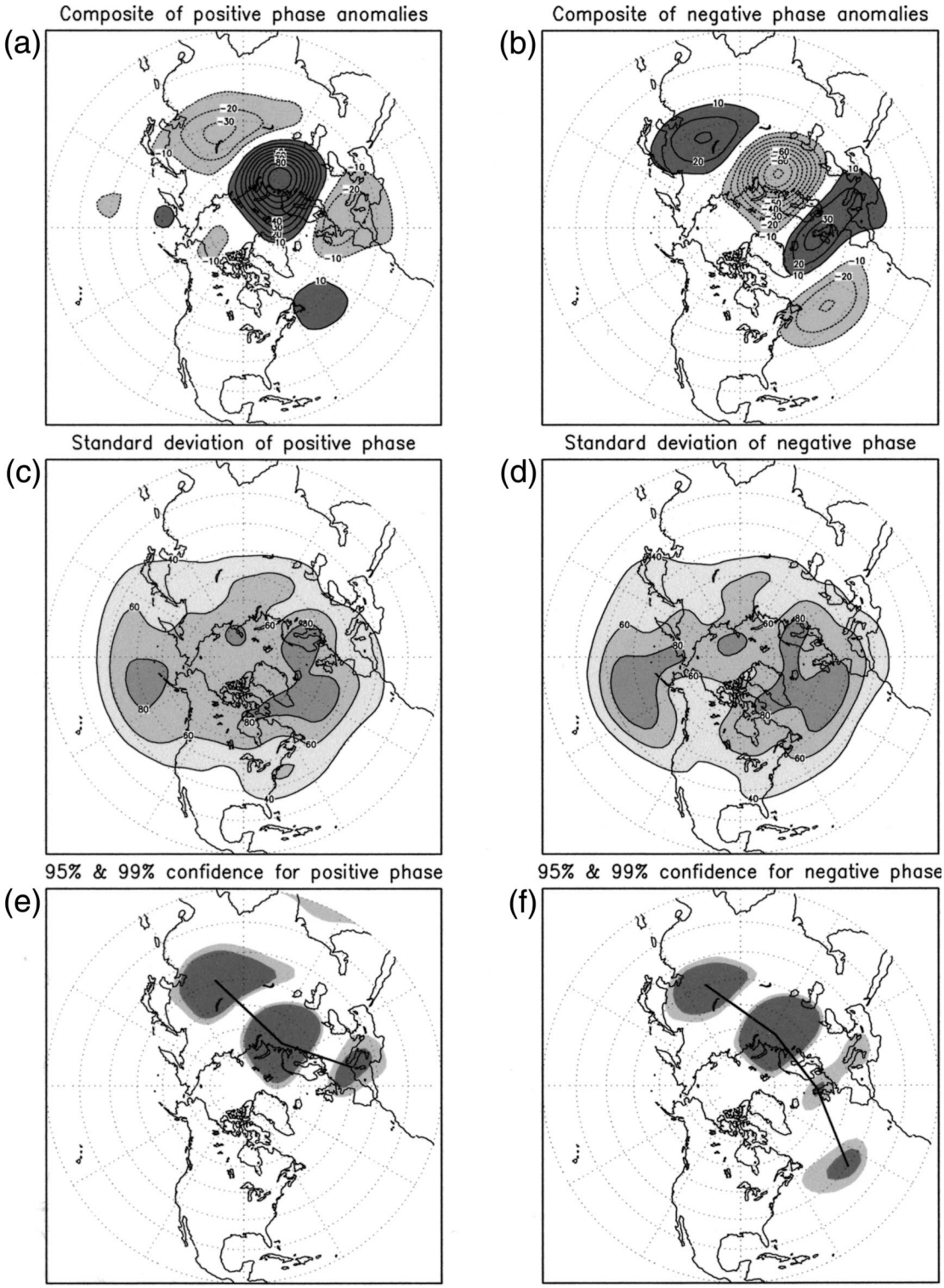

FIG. 5. The same as Fig. 2 except for an action center located in western Russia. The domain, as marked in Fig. 1, is 55°–67.5°N, 40°–82.5°E.

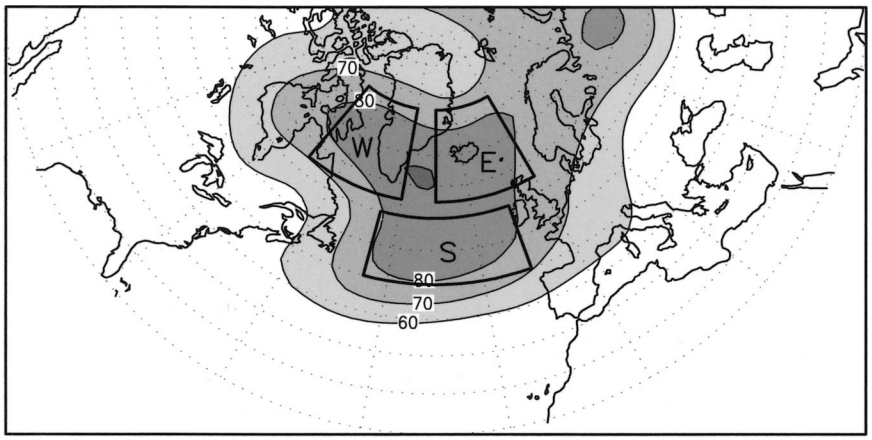

FIG. 6. The same std dev chart as shown in Fig. 1, except for the North Atlantic basin, for the marking of three regions used as bases for the construction of teleconnection composites for Figs. 7–9. The details of the three domains can be found in Figs. 7–9.

composites is emphasized here with a straight line connecting the two downstream action centers. We see that for the positive composite (Fig. 2e) the two downstream centers are located in the interior of North America, while for the negative composite (Fig. 2f) the southernmost downstream action center shifts far eastward into the western Atlantic. Other interesting features to note are 1) for the positive composite, it is clear that the significant area at the southern U.S. center, as well as the subtropical North Pacific center, is much more extensive than for the negative composite, 2) both composites (Figs. 2a,b) show contours in the North Atlantic; however, they are not statistically significant, as revealed in Figs. 2e and 2f, and 3) the orientation of the significant area at the downstream action center is distinct: more zonal flow, as an extension of the Bermuda high, for the positive composite, while more meridional flow for the negative composite, resulting from the couplet of the Canadian high and the mid-Atlantic coastal low (for monthly mean data).

As shown above, structurally, the two southernmost action centers display some difference: more zonal in orientation versus more meridional. Also, the positive composites are seen to be much more significant, covering much larger regions. Ignoring the issue of structural difference for the moment, one could ask whether the positive and negative composites are truly different statistically; that is, is there a nonlinearity in this teleconnection beyond sampling error? The result of this test indicates that the sum (or the difference, after adjusting for sign change) of positive and negative composites now covers a much smaller region over the south-central states of the United States (not shown), and, because of the much-reduced difference in absolute magnitude, the statistical significance reduces to only about 80%. Besides showing whether nonlinearity is statistically significant, the combined sum (or difference) loses distinct features that might suggest a difference in physical processes. Based on this rationale, we prefer to present the structure and statistical significance separately for the positive and negative composites.

c. Sensitivity of North Atlantic–based teleconnections

Results similar to those in Fig. 2 were obtained for teleconnections based on the North Atlantic std dev maximum and these are shown in Fig. 3. For this sector, the domain used, as shown in Fig. 1, is 55°–72.5°N, 10°–60°W, which covers most of the northern part of the std dev maximum with values greater than 70 m. The selection of this domain needs a little bit of explanation. It is well known that there is a frequent and strong north–south standing oscillation in this sector. In fact, the std dev chart in Fig. 1 gives a hint of this north–south standing oscillation and its likely nodal line, which can be detected by the existence of a weak std dev minimum along 55°N. The existence of this minimum implies the likelihood of two std dev maxima straddling the nodal line. These two maximum regions are located so closely together that they appear as a large region of std dev maximum. The teleconnection structures based on the region south of 55°N deserve a separate treatment, which we will present in a later section. Meanwhile, the domain selected for compositing in this section includes the North Atlantic std dev absolute maximum.

Again, the statistical significance of the resulting teleconnections, as shown in Figs. 3e and 3f, displays certain disparity. With a straight line connecting two action centers in each panel to emphasize the major difference, we see that for the positive composite the teleconnection is mainly over the North Atlantic, while for the negative composite a stronger teleconnection is toward central Europe. It is interesting to note that over central Europe there is no significant teleconnection for the positive

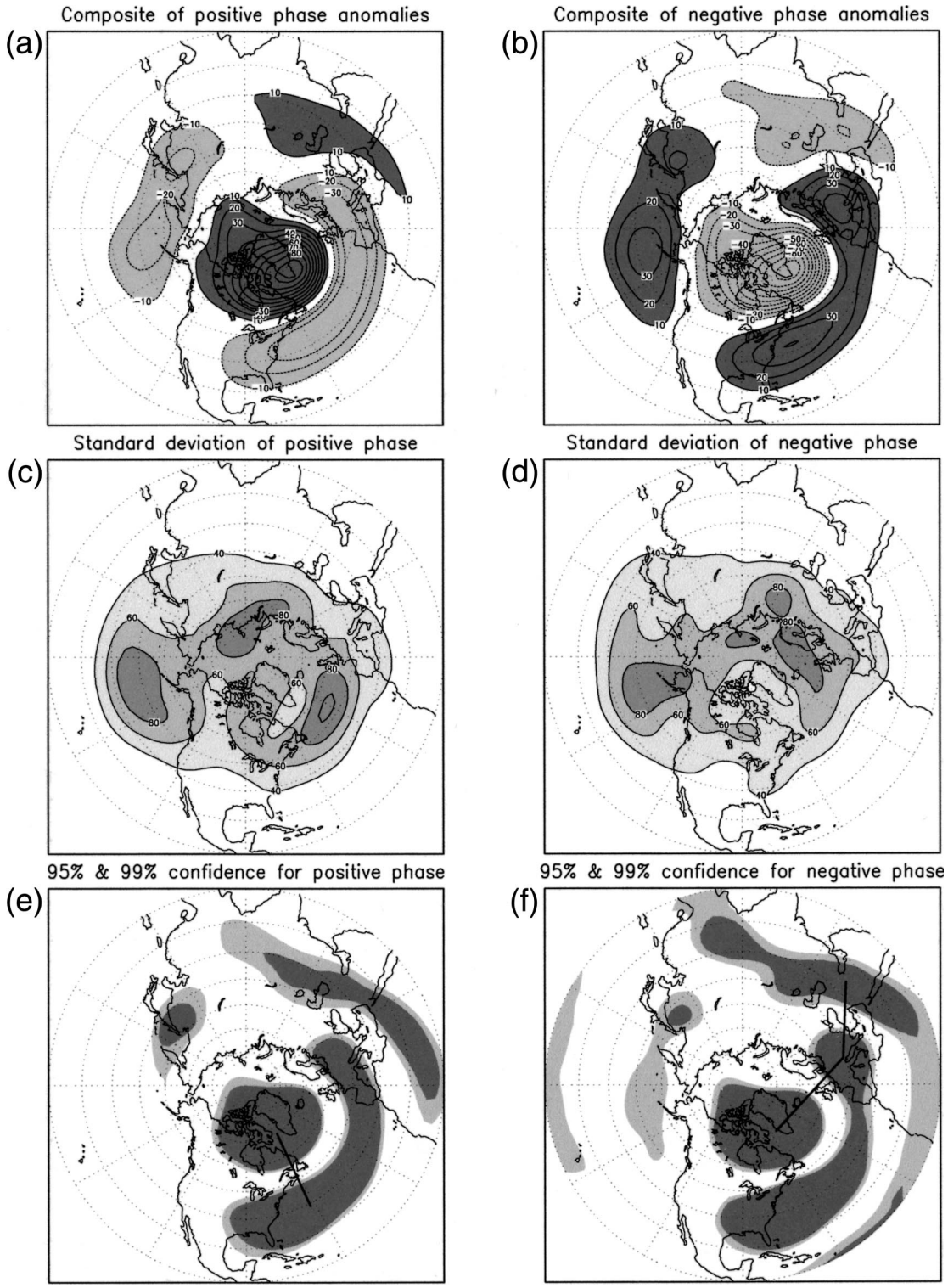

FIG. 7. The same as Fig. 2 except for an action center located in the western domain of the North Atlantic. The domain, as marked in Fig. 6, is 57.5°–72.5°N, 70°–40°W.

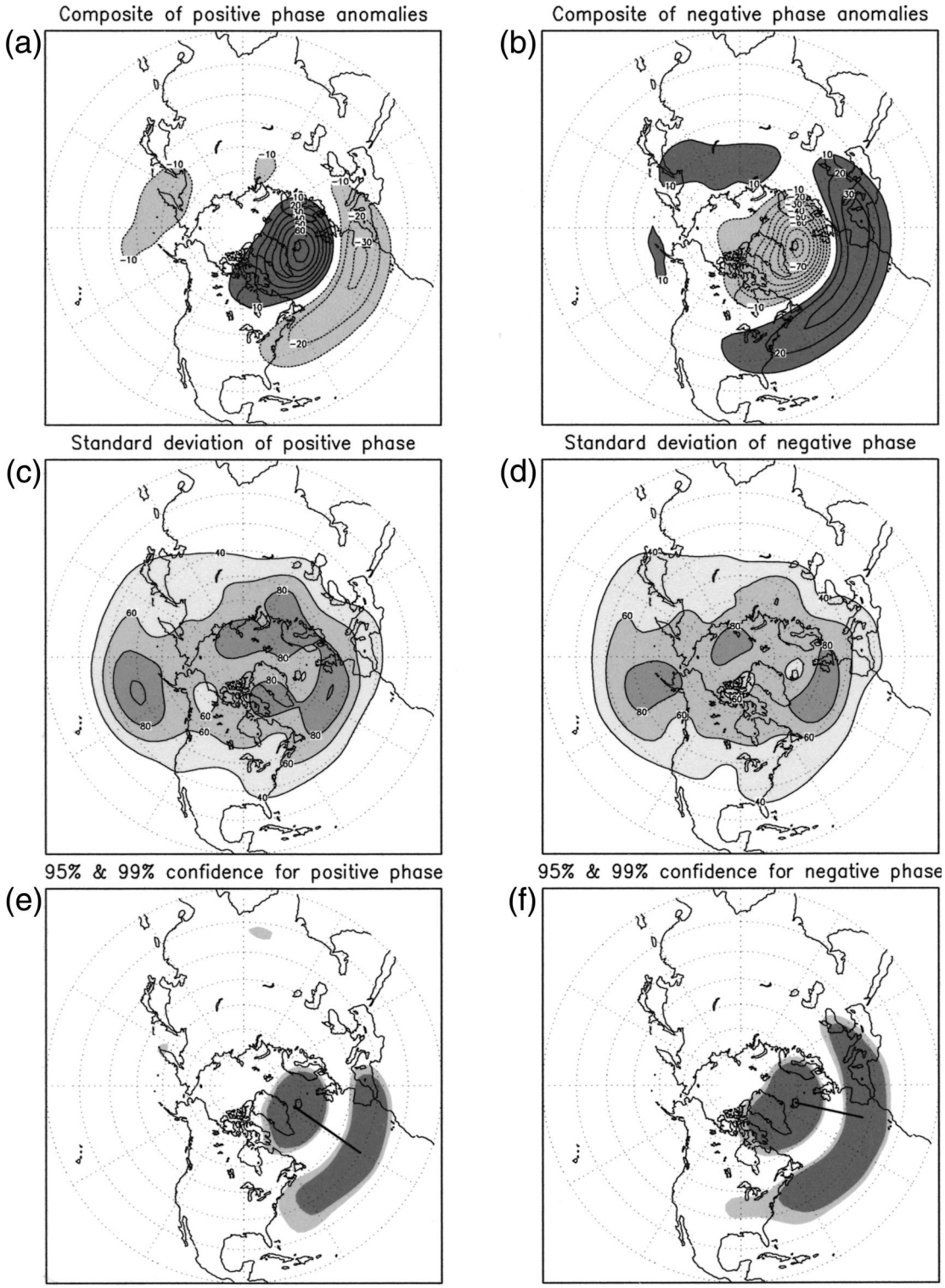

FIG. 8. The same as Fig. 7 except for an action center located in the eastern domain of the North Atlantic. The domain, as marked in Fig. 6, is 57.5°–72.5°N, 30°W–0°.

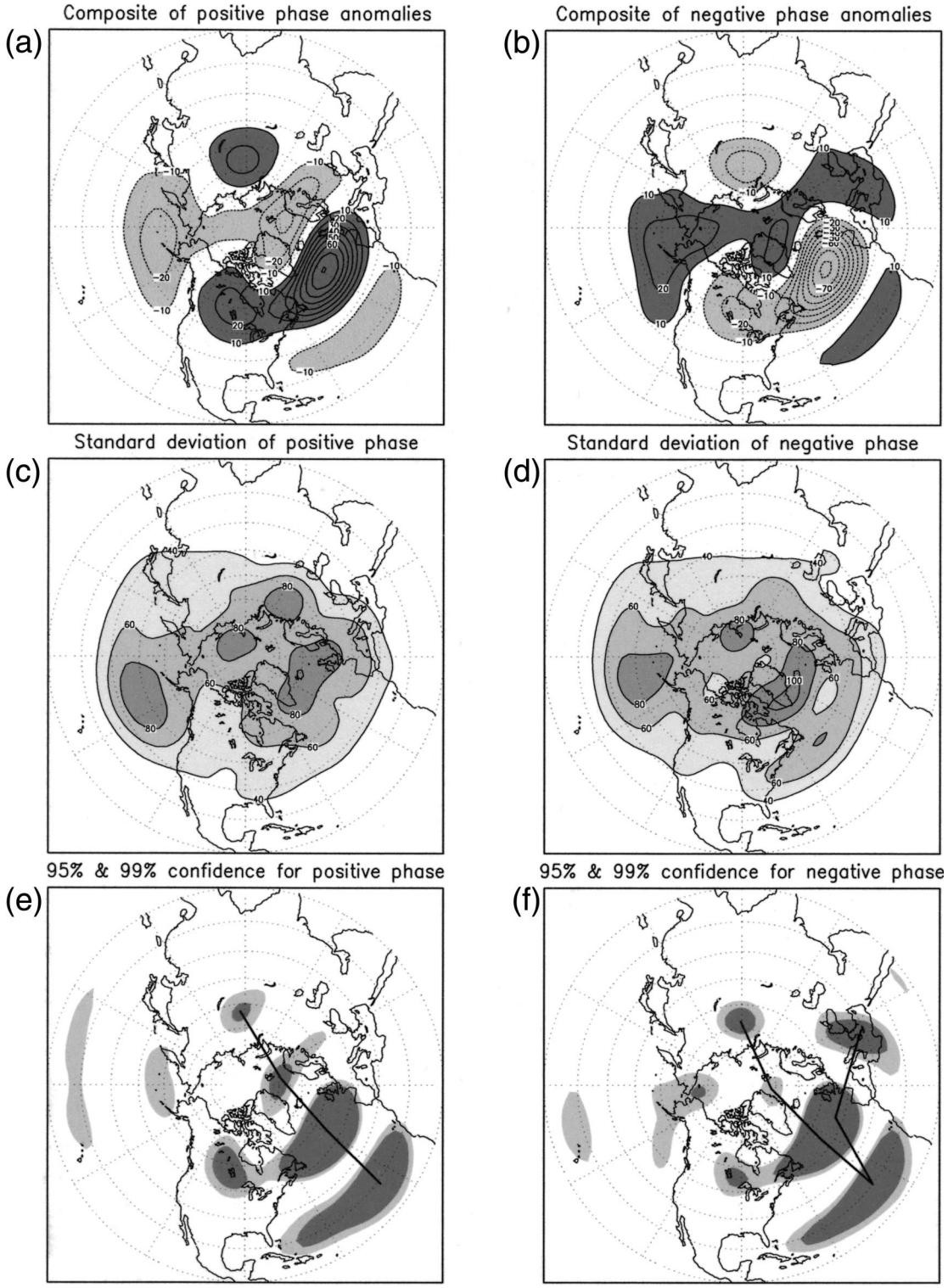

FIG. 9. The same as Fig. 7 except for an action center located in the southern domain of the North Atlantic. The domain, as marked in Fig. 6, is 45°–55°N, 45°–10°W.

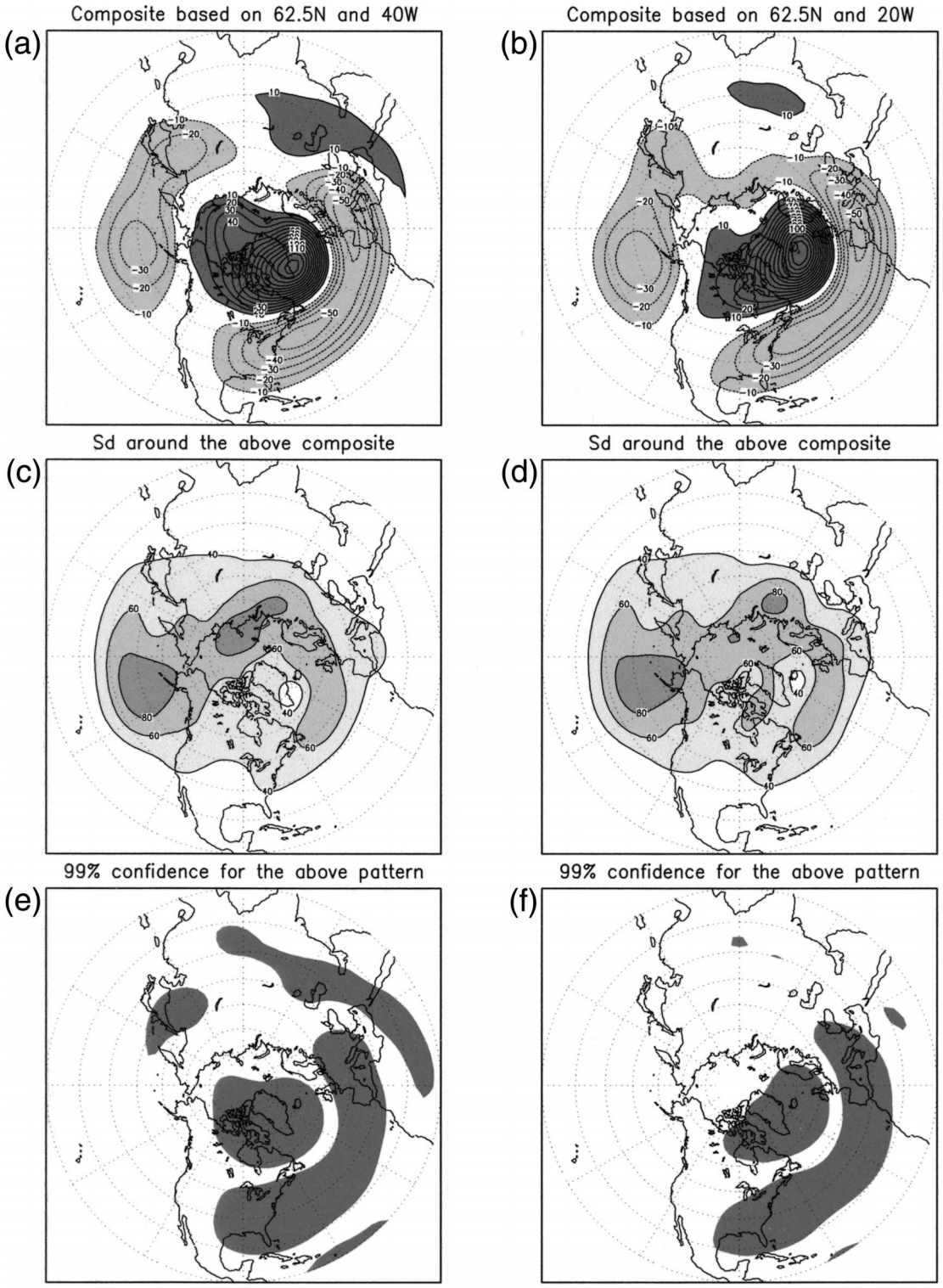

FIG. 10. Comparison of teleconnection structures and their 99% confidence level in statistical significance. (a), (c), (e) The teleconnection is based on 62.5°N and 40°W and (b), (d), (f) is based on 62.5°N and 20°W. Contours are similar to those in Fig. 2.

composite (Fig. 3e). For the negative composite, the teleconnection over the North Atlantic is also prominent. Although the composites (Figs. 3a,b) also show contours over the North Pacific, they are not significant, except for a tiny area near the Kamchatka Peninsula, as shown in Figs. 3e and 3f.

d. Sensitivity of Arctic standard deviation-maximum-based teleconnections

As shown in Fig. 1, there is a std dev maximum inside the Arctic Circle, at about 82.5°N, 120°E. This Arctic std dev maximum also shows up in the std dev charts of Blackmon et al. (1984a) and Kushnir and Wallace (1989). Results similar to Figs. 2 and 3 were obtained for this Arctic std dev-maximum-based teleconnection and are shown in Fig. 4. The domain used for these results is 75°–87.5°N, 65°–175°E, as shown in Fig. 1, and encloses all standard deviations with magnitudes larger than 80 m. The main disparity between the resulting teleconnections can be observed in Figs. 4e and 4f. The positive composite appears to have a significant northeastern Pacific teleconnection action center, which is entirely missing in the negative composite.

e. Sensitivity of western Russia standard deviation-maximum-based teleconnections

A noticeable difference between our std dev chart (Fig. 1) and the earlier ones in Blackmon et al. (1984a) and Kushnir and Wallace (1989) is the existence of a std dev maximum over western Russia, near 62°N, 54°E. As mentioned earlier, our data is from the period 1971 to 2001, while the earlier analyses were based on the period from 1963 to 1980. Since this std dev maximum is comparable in magnitude to the other three, we would like to see its teleconnections as well. Also, we would like to examine whether there is a prominent asymmetry characteristic between the opposite phases of its teleconnection pattern. Again, results similar to Figs. 2 and 3 are obtained for this western Russia std dev-maximum–based teleconnection. The results are shown in Fig. 5. The domain used for these results is 55°–67.5°N, 40°–82.5°E, as shown in Fig. 1, and encloses all standard deviations with values larger than 80 m. As shown in Fig. 5, prominent wave train teleconnections can be observed. In Figs. 5e and 5f, the main disparities between positive and negative teleconnections are 1) wave trains with three action centers versus one with four action centers, 2) the track of the wave trains appears to be bending in the opposite direction, concaving equatorward versus poleward, and 3) the positive composites show characteristics of omega-type of blocking formation, while the negative composites show wave train structures, possibly playing a role in two-dimensional Rossby wave dispersion, as described by Blackmon et al. (1984a).

f. Further investigation of teleconnections based on different regions in the North Atlantic

As shown in Fig. 1, large variances spread over nearly the entire North Atlantic. And, as shown in Blackmon et al. (1984a), a teleconnection based on a different region can show a different structure. In this section, we investigate the sensitivity of statistical significance of teleconnections based on different regions of the North Atlantic. Figure 6 shows the three regions that the results are based on. The teleconnections associated with each region will be referred to as WATL, EATL, and SATL, for the western, eastern, and southern North Atlantic, respectively. The domains used, as shown in Fig. 6, are 57.5°–72.5°N, 70°–40°W for the western region, 57.5°–72.5°N, 30°W–0° for the eastern region, and 45°–55°N, 45°–10°W for the southern region.

Figures 7a and 7b show the WATL teleconnection composites and Figs. 7e and 7f show their respective 95% and 99% confidence levels. Careful inspection again reveals, as shown in Fig. 3, that the negative composite shows much better teleconnection to western Europe. Similar features can also be observed for the EATL teleconnections, as shown in Fig. 8. In general, as shown in panels a and b of Figs. 7 and 8, the negative composites appear to have better statistical significance.

There is a dramatic difference in structure between the WATL and EATL teleconnections. While the WATL patterns are strikingly similar to the Arctic (Annular) Oscillation, reported by Thompson and Wallace (1998, 2000) and Baldwin and Dunkerton (1999), the EATL patterns are essentially the same as the classical North Atlantic Oscillation (Walker and Bliss 1932; van Loon and Rogers 1978). Comparing panels a and b of Figs. 7 and 8, the WATL teleconnections show a wide spread of high significance over a large portion of the Northern Hemisphere, in sharp contrast to a rather restricted region of high significance in the North Atlantic for the EATL patterns. More features will be described in the next section.

Figure 9 shows the results of the SATL teleconnections and their significance patterns. Based on the SATL region, the teleconnections assume a wave train structure. An inspection reveals right away that there is a disparity between the positive and negative composites. While the large positive anomalies in the SATL region tend to result in only one-track wave trains (Fig. 9e), the large negative anomalies over the same region are likely to yield two-track wave trains (Fig. 9f). Again, the negative composite shows teleconnection to the European sector, while the positive composite stays within the North Atlantic, as shown in Figs. 3 and 8.

g. Sensitivity of teleconnection structure to a slight shift in base point in the North Atlantic

The dramatic difference in structure between the WATL and EATL teleconnections can be brought to

sharper focus by a side-by-side comparison, as shown in Fig. 10. In this figure we are not making a comparison of asymmetry characteristics between the positive and negative composites, but are displaying a large sensitivity in teleconnection structure to a slight change in their respective base points. Specifically, with a slight shift in base point, at the high latitude of 62.5°N, from 40° to 20°W, two teleconnections in linear form were constructed. This time, the selection criterion is for an anomaly at base point (not within a domain) to be larger than 100 m, either in positive or negative sign. As shown in Figs. 10e and 10f, the teleconnection structures turn out to be dramatically different. The sensitivity of the teleconnection structure to a slight shift in base point can indeed be large. In this case, a hemispherical Annular Oscillation pattern versus a regional North Atlantic Oscillation pattern is observed, with a distinct statistical significance pattern to support the dramatic difference.

4. Conclusions

Some of the well-known teleconnection patterns are examined here for their sensitivity to a sign change at their respective primary action center as well as to a slight shift in the base point. There are prominent nonlinear characteristics between the opposite phases of a teleconnection pattern. These asymmetry properties should be utilized to enhance a long-range prediction application.

The PNA pattern exhibits significant teleconnection over the interior of North America for large positive anomalies over the North Pacific, while their opposite large negative anomalies tend to result in teleconnections extending to the western region of the North Atlantic. In the North Atlantic sector, the general situation is that, for large positive anomalies, teleconnection is more likely to form over the North Atlantic, while for large negative anomalies, it is likely to form over the Europe sector as well. Also, when based on the central North Atlantic area, large positive anomalies are more likely to form one-track wave trains, while large negative anomalies are more likely to produce two-track wave trains.

Also, in the North Atlantic, the structure of a teleconnection can be highly regionally dependent, as reported by Blackmon et al. (1984a). Along this line, we find striking similarity between our WATL pattern and the Arctic (Annular) Oscillation and an essential similarity between our EATL pattern and the classical North Atlantic Oscillation. Both teleconnection patterns are highly significant, with confidence levels beyond 99%.

Sensitivity of teleconnection structure to a slight shift in base point can be fairly large in the North Atlantic.

REFERENCES

Ambaum, M. H. O., and B. J. Hoskins, 2002: The NAO troposphere–stratosphere connection. *J. Climate,* **15,** 1969–1978.

Baldwin, M. P., and T. J. Dunkerton, 1999: Propagation of the Arctic Oscillation from the stratosphere to the troposphere. *J. Geophys. Res.,* **104,** 30 937–30 946.

Barnston, A. G., and R. E. Livezey, 1987: Classification, seasonality and persistence of low-frequency atmospheric circulation patterns. *Mon. Wea. Rev.,* **115,** 1083–1126.

Blackmon, M. L., Y. H. Lee, and J. M. Wallace, 1984a: Horizontal structure of 500 mb height fluctuations with long, intermediate and short time scales. *J. Atmos. Sci.,* **41,** 961–980.

——, ——, ——, and H. H. Hsu, 1984b: Time variation of 500 mb height fluctuations with long, intermediate and short time scales as deduced from lag-correlation statistics. *J. Atmos. Sci.,* **41,** 981–992.

Deser, C., and M. L. Blackmon, 1993: Surface climate variations over the North Atlantic Ocean during winter: 1900–1993. *J. Climate,* **6,** 1743–1753.

Hurrell, J. W., 1995a: Transient eddy forcing of the rotational flow during northern winter. *J. Atmos. Sci.,* **52,** 2286–2301.

——, 1995b: Decadal trends in the North Atlantic Oscillation regional temperatures and precipitation. *Science,* **269,** 676–679.

——, 1996: Influence of variations in extratropical wintertime teleconnections on Northern Hemisphere temperatures. *Geophys. Res. Lett.,* **23,** 665–668.

——, and H. van Loon, 1997: Decadal variations in climate associated with the North Atlantic Oscillation. *Climatic Change,* **36,** 301–326.

Kalnay, E., and Coauthors, 1996: The NCEP/NCAR 40-Year Reanalysis Project. *Bull. Amer. Meteor. Soc.,* **77,** 437–471.

Kushnir, Y., 1994: Interdecadal variations in North Atlantic sea surface temperature and associated atmospheric conditions. *J. Climate,* **7,** 142–157.

——, and J. M. Wallace, 1989: Low-frequency variability in the Northern Hemisphere winter: Geographical distribution, structure and time-scale dependence. *J. Atmos. Sci.,* **46,** 3122–3142.

——, V. J. Cardone, J. G. Greenwood, and M. Cane, 1997: On the recent increase in North Atlantic wave heights. *J. Climate,* **10,** 2107–2113.

Lorenz, E. N., 1951: Seasonal and irregular variations of the Northern Hemisphere sea-level pressure profile. *J. Meteor.,* **8,** 52–59.

Mo, K. C., and R. E. Livezey, 1986: Tropical–extratropical geopotential height teleconnections during the Northern Hemisphere winter. *Mon. Wea. Rev.,* **114,** 2488–2515.

Morrison, D. F., 1983: *Applied Linear Statistical Methods.* Prentice Hall, 562 pp.

Nakamura, H., 1996: Year-to-year and interdecadal variability in the activity of intraseasonal fluctuations in the Northern Hemisphere wintertime circulation. *Theor. Appl. Climatol.,* **55,** 19–32.

Namias, J., 1981: Teleconnections of 700mb height anomalies for the Northern Hemisphere. *California Cooperative Oceanic Fisheries Investigations Atlas 29,* Scripps Institution of Oceanography, 265 pp.

O'Connor, J. F., 1969: Hemispheric teleconnections of mean circulation anomalies at 700 millibars. ESSA Tech. Rep. WB10, 103 pp.

Shabbar, A., K. Higuchi, W. Skinner, and J. L. Knox, 1997: The association between the BWA index and winter surface temperature variability over eastern Canada and west Greenland. *Int. J. Climatol.,* **17,** 1195–1210.

Thompson, D. W. J., and J. M. Wallace, 1998: The Arctic Oscillation signature in the wintertime geopotential height and temperature fields. *Geophys. Res. Lett.,* **25,** 1297–1300.

——, and ——, 2000: Annual modes in the extratropical circulation. Part I: Month-to-month variability. *J. Climate,* **13,** 1000–1016.

Van den Dool, H. M., S. Saha, and A. Johansson, 2000: Empirical orthogonal teleconnections. *J. Climate,* **13,** 1421–1435.

van Loon, H., and J. C. Rogers, 1978: The seesaw in the winter temperatures between Greenland and northern Europe. Part I: General description. *Mon. Wea. Rev.,* **106,** 296–310.

Visbeck, M., H. Cullen, G. Krahmann, and N. Naik, 1998: An ocean

model's response to North Atlantic Oscillation–like wind forcing. *Geophys. Res. Lett.*, **25,** 4521–4524.
Walker, G. T., and E. W. Bliss, 1932: World weather V. *Mem. Roy. Meteor. Soc.*, **4,** 53–84.
Wallace, J. M., and D. S. Gutzler, 1981: Teleconnections in the geopotential height field during the Northern Hemisphere winter. *Mon. Wea. Rev.*, **109,** 784–812.
Walsh, J. E., W. L. Chapman, and T. L. Shy, 1996: Recent decrease of sea level pressure in the central Arctic. *J. Climate*, **9,** 480–486.